Hydrophobic surfaces for enhanced differentiation of embryonic stem cell-derived embryoid bodies

Bahram Valamehr*, Steven J. Jonas†, Julien Polleux†, Rong Qiao*‡, Shuling Guo§¶, Eric H. Gschweng‖, Bangyan Stiles*, Korey Kam†, Tzy-Jiun M. Luo†, Owen N. Witte*§¶‖**, Xin Liu*‡, Bruce Dunn†¶**, and Hong Wu*¶**

*Department of Molecular and Medical Pharmacology, David Geffen School of Medicine, †Department of Materials Science and Engineering, Henry Samueli School of Engineering and Applied Sciences, ‡Department of Pathology and Laboratory Medicine and Embryonic Stem Cell/Transgenic Mice Shared Resource, §Department of Microbiology, Immunology, and Molecular Genetics, ¶Eli and Edythe Broad Center of Regenerative Medicine and Stem Cell Research, and ‖Howard Hughes Medical Institute, University of California, Los Angeles, CA 90095

Contributed by Owen N. Witte, July 25, 2008 (sent for review October 17, 2007)

With their unique ability to differentiate into all cell types, embryonic stem (ES) cells hold great therapeutic promise. To improve the efficiency of embryoid body (EB)-mediated ES cell differentiation, we studied murine EBs on the basis of their size and found that EBs with an intermediate size (diameter 100–300 μm) are the most proliferative, hold the greatest differentiation potential, and have the lowest rate of cell death. In an attempt to promote the formation of this subpopulation, we surveyed several biocompatible substrates with different surface chemical parameters and identified a strong correlation between hydrophobicity and EB development. Using self-assembled monolayers of various lengths of alkanethiolates on gold substrates, we directly tested this correlation and found that surfaces that exhibit increasing hydrophobicity enrich for the intermediate-size EBs. When this approach was applied to the human ES cell system, similar phenomena were observed. Our data demonstrate that hydrophobic surfaces serve as a platform to deliver uniform EB populations and may significantly improve the efficiency of ES cell differentiation.

hydrophobicity | self-assembled monolayers | serum-free differentiation

The potential of embryonic stem (ES) cells to differentiate into all specialized cell types has made them attractive models for studying the mechanisms of lineage commitment and has opened pathways for regenerative medicine (1). Various *in vitro* strategies have been developed for differentiation of ES cells into populations of specific cell types (2). Of these strategies, the formation of three-dimensional cell aggregates known as embryoid bodies (EBs) is a common and critical intermediate to the induction of lineage-specific differentiation (3, 4). In addition, lineage differentiation programs within the EB closely resemble lineage commitment *in vivo* in the developing embryo, further highlighting the importance of the ES cell–EB culture system (5–8).

Although EBs can be generated through several methodologies, the suspension culture technique allows for easy access to the cultured EBs and can be scaled for expansion (9). In this method, EBs are formed when ES cells are removed from feeder contact and dispersed on low-attachment tissue culture plates, supplemented by culture medium absent of key factors necessary for the maintenance of undifferentiated ES cell growth. Low-attachment tissue culture plates typically use neutral, hydrophilic hydrogels to prevent protein adsorption and subsequent cell attachment, facilitating the initial aggregation of ES cells that is critical to EB formation (10). The cellular aggregates formed by this procedure will develop simple EBs that consist of an outer layer of endoderm cells within 2–4 days (3). At this point, two differentiation strategies can be applied. If suspension culture is continued, simple EBs will differentiate further to form cystic EBs that typically contain an inner layer of columnar ectoderm-like cells and that accumulate fluid in the interior of the structure (3). However, the most commonly used multistage differentiation protocols use the second strategy in which simple EBs are transferred onto adherent tissue culture surfaces after day 4 of EB development and are subsequently supplemented with key factors necessary for lineage-specific differentiation (5, 8, 11). One shortcoming of this suspension culture system is the production of heterogeneous EBs, varying in size and morphology, which may limit homogeneous differentiation and impede production yields (12–15).

In this study, we investigated alternative surface conditions to promote uniform EB formation and enhance the differentiation yields of ES cells. Indeed, altering surface properties is known to significantly affect cell growth, attachment, and differentiation in various culture systems (16–19). For example, by using a polyacrylamide gel in which Young's Modulus could be tuned based on the degree of cross-linking, Engler *et al.* (17) provided compelling evidence that matrix elasticity can specify lineage commitment toward neurons, myoblasts, and osteoblasts. Our findings demonstrate the benefit of using hydrophobic surfaces for monodispersed EB formation. The materials tested in our study, such as polydimethylsiloxane (PDMS) or self-assembled-monolayer (SAM) surfaces presenting terminal hydrophobic moieties, are easily adapted by, and widely accessible to, the general research community, which should enable more laboratories to better pursue ES cell research.

Results

EB Size Determines Cellular Viability, Proliferation, and Differentiation Potential. EBs produced in suspension culture are known to be heterogeneous in size and morphology. However, how EB size and morphology influence subsequent differentiation and production yield is not clear. To understand this critical issue, we conducted a systematic study by first manually separating day 4 murine EBs into three subpopulations based on their diameter: small (<100 μm), intermediate (100–300 μm), and large (>300 μm) (Fig. 1*A*). We then compared their respective potentials for cellular survival, proliferation, and differentiation of these three subpopulations.

Cellular survival can be determined by monitoring the percentage of cells undergoing apoptosis. Indicated by annexin V (AV) and propidium iodide (PI) positive staining, apoptosis can be categorized into three temporal stages: early (AV^+/PI^-), intermediate (AV^+/PI^+), and late (AV^-/PI^+) (20). Very little late-stage apoptosis was detected during day 4 of EB formation for all three subgroups [supporting information (SI) Fig. S1*A*].

Author contributions: B.V., S.J.J., J.P., S.G., E.H.G., B.S., K.K., T.-J.M.L., O.N.W., B.D., and H.W. designed research; B.V., S.J.J., J.P., R.Q., S.G., E.H.G., and K.K. performed research; B.V., S.J.J., J.P., S.G., E.H.G., B.S., O.N.W., X.L., B.D., and H.W. analyzed data; and B.V., S.J.J., J.P., S.G., E.H.G., O.N.W., X.L., B.D., and H.W. wrote the paper.

The authors declare no conflict of interest.

**To whom correspondence may be addressed. E-mail: hwu@mednet.ucla.edu, bdunn@ucla.edu, or owenw@microbio.ucla.edu.

This article contains supporting information online at www.pnas.org/cgi/content/full/0807235105/DCSupplemental.

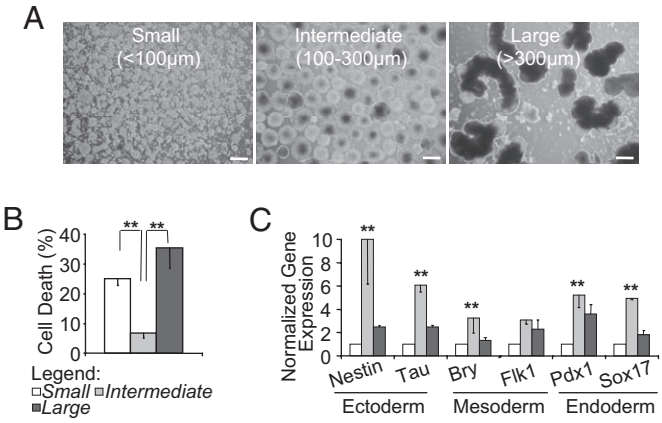

Fig. 1. EB size influences cellular viability, proliferation, and differentiation potential. (*A*) Day 4 EBs were manually separated into three size categories: small, intermediate, and large. (Scale bars, 250 μm.) (*B*) EBs of the intermediate size contain the lowest number of apoptotic cells. $n = 3$. (*C*) qRT-PCR analysis of lineage marker expression for ectoderm (Nestin and Tau), mesoderm [Brachyury (Bry) and Flk1], and endoderm (Pdx1 and Sox17) in each subpopulation. The level of 18S serves as an internal control. $n = 3$. Data presented as mean ± SD. **, $P \leq 0.01$.

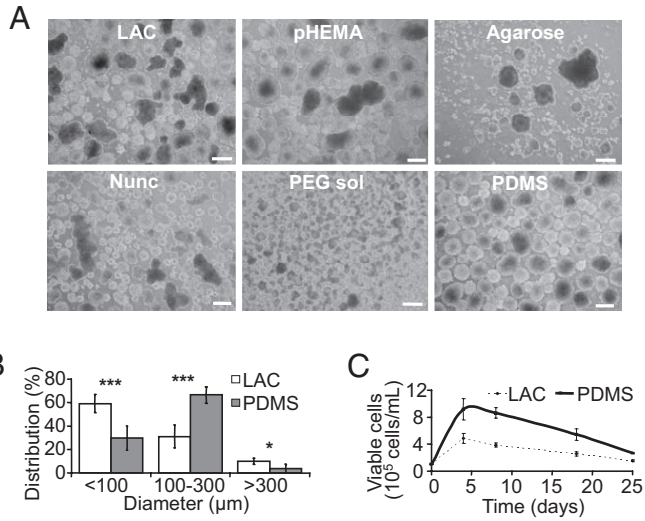

Fig. 2. PDMS promotes intermediate-size EB formation. (*A*) Parallel comparison of day 4 EB formation on various biocompatible surfaces. (Scale bars, 250 μm.) (*B*) PDMS-coated surface enriches for the intermediate-size EBs. The diameters of day 4 EBs were measured. $n = 4$. (*C*) Enrichment for the intermediate-size EBs on PDMS-coated surface results in increased number of viable cells. EBs were monitored in continuous culture by sampling a subset of EBs at indicated time points; viable cells were counted after trypan blue staining and plotted over a 25-day culture period. $n = 5$. Data presented as mean ± SD; *, $P \leq 0.05$; ***, $P \leq 0.001$.

This observation was confirmed independently with 7-amino-actinomycin D staining (data not shown), indicating that during the first stage of EB formation, the majority of the compromised cells have only entered the initial stages of apoptosis. When all stages of apoptosis were considered, the intermediate-size EB subgroup had 3- and 5-fold fewer apoptotic cells (6.7%; $P \leq 0.01$) than the small (25.0%) and large (35.5%) EB populations, respectively (Fig. 1*B* and Fig. S1*A*).

To address whether EB size can also influence cellular proliferation, we evaluated proliferation rates by using flow cytometry-mediated cell cycle analysis because percentage population in G_0/G_1 is inversely, and in G_2/M is directly, correlated to the cellular proliferation rate. The large-EB subgroup contains a reduced number of cells residing in G_2/M (15.3%; $P \leq 0.01$) but an increased number in G_0/G_1 (53.0%; $P \leq 0.01$) cell cycle phase, relative to small and intermediate-size EBs, suggesting that large EBs are the least proliferative subpopulation (Fig. S1*B*). Differences in cell cycle distribution between small- and intermediate-size EB subgroups are marginal but remain statistically significant ($P \leq 0.05$).

In addition to cellular proliferation and viability, EB size also influences differentiation potential. Upon differentiation, EBs begin to express genes associated with the three somatic lineages: ectoderm, endoderm, and mesoderm (21). We therefore examined the expression levels of genes associated with lineage differentiation in each subpopulation. Quantitative reverse-transcription–polymerase chain reaction (qRT-PCR) analysis revealed that EBs of intermediate size express the highest levels of those genes associated with lineage differentiation (Fig. 1*C* and Table S1). Small EBs display a significant attenuation of gene expression for all three somatic lineages, whereas gene expression levels of the large-EB subgroup fall in between (Fig. 1*C*). These findings thus demonstrate that intermediate-size EBs are the most proliferative, display the lowest rate of cell death, and may have the greatest differentiation potential.

Surface Chemical Properties Influence EB Formation. In an attempt to enrich for EBs of the preferred size, we surveyed several biocompatible coatings, such as agarose, polyethylene glycol silica sol gel (PEG sol), polyhydroxyethylmethacrylate (pHEMA), and polydimethylsiloxane (PDMS) (Table S2). Two commonly used tissue culture plates—low-binding culture plates (Nunc) and ultra-low-attachment culture (LAC; Corning) plates—were also incorporated into the study (Fig. 2*A*). These surfaces were selected based on their neutral charge and their ability to resist cellular adhesion and spreading, which is a principal requirement for suspension culture. The major differences among these surfaces are the terminal functional group and hydrophobicity, which can be assessed by water contact angle; contact angles >90° are considered hydrophobic. By varying these two parameters, we tested whether surface chemical properties could influence EB formation.

When an equal number of murine ES cells from the same stock were plated onto the abovementioned surfaces, a variety of EB sizes and morphologies were observed (Fig. 2*A*). Interestingly, PDMS—the sole hydrophobic surface in our study—promoted the development of EBs that were more uniform in size, with a reduction in cellular clumps and debris (Fig. 2*A Lower Right*). Based on the results seen in this initial screen, we decided to perform an in-depth study of the PDMS-coated surface.

PDMS Surface Promotes Formation of Intermediate-Size EBs. When we compared EBs formed on PDMS-coated surfaces with EBs derived from LAC plates—which are routinely used for EB formation—we found that PDMS surfaces promoted the formation of intermediate-size EBs by >2-fold (Fig. 2*B*). To confirm that this finding was not cell line-dependent, other independent ES cell lines were subjected to the same test and analyzed during the first 4 days of differentiation (Fig. S2). During day 1 of differentiation, cell aggregates formed on LAC plates varied in size and shape, with visible large clumps (Fig. S2*A*), whereas aggregates developed on PDMS appeared to be similar in shape and size and evenly distributed throughout the culture well (Fig. S2*B*). This even distribution, combined with a reduction in debris and larger aggregates, translated to morphologically uniform EBs after 4 days of culture (Fig. S2 *C–H*), suggesting that PDMS surfaces may better support EB development (22–24).

Further study revealed an increase in total viable cells on PDMS as compared with EBs derived from LAC plates during 25 days of continuous EB culture, with a 2-fold increase at day

8 (Fig. 2*C*). The increase in total viable cells also coincides with the period when the majority of commitment toward all three germ cell layers and the appearance of specialized cell types are detected during EB-mediated cell differentiation (1, 2, 7, 25–27). In addition, the percentage of cells in G_0/G_1 cell cycle phase was lower in EBs formed on PDMS (36.2%; $P \leq 0.01$) than in EBs formed on LAC (42.8%) (Fig. S3*A*). The decrease in G_0/G_1 and increase in $S/G_2/M$ phases displayed by EBs formed on PDMS held true at days 4, 8, and 16 of EB development (Fig. S3*A*). Furthermore, EBs formed on PDMS exhibited increased total metabolic activity, consistent with increased cell viability and proliferation (Fig. S3*B*).

We then used three primer sets per germ layer to monitor EB differentiation over time. In general, these lineage-specific differentiation markers appeared earlier and sustained longer in EBs formed on PDMS than in their counterparts formed on LAC plates (Fig. S3*C*). We next studied whether EBs formed on PDMS readily undergo hematopoietic differentiation by assessing the presence of hematopoietic progenitors by means of quantitative FACS analysis and methylcellulose assay. Similar to a previous report (28), we observed a sequential appearance of Flk1- and c-Kit-positive populations in day 4 EBs, then CD34- and CD45-positive populations in day 7 EBs. To this extent, FACS analysis reveals that $Flk1^+$, $CD45^+$, and $CD34^+$ populations are significantly increased in EBs generated on PDMS, as compared with those on LAC plates (Fig. S3*D*). When day 7 EBs were dissociated and plated in methylcellulose (Stem Cell Technologies), we also detected a 4.3-fold increase in the number of hematopoietic colonies (Fig. S3*E*), suggesting that EBs formed on PDMS indeed have greater differentiation potential.

Role of Hydrophobicity in EB Formation. By analyzing the surface properties of the materials used, we found that one potential determining factor for uniform EB formation may be surface hydrophobicity (Table S2). To test whether hydrophobicity plays a critical role in controlling EB size distribution, we used SAMs of alkanethiolates on gold-coated substrates as model surfaces (29). We chose to vary the alkyl chain length of the SAM films, where longer chained alkanethiol structures (R in Fig. 3*A*) would lead to increases in hydrophobicity at the cell culture interface as measured by the contact angle (θ in Fig. 3*A*). SAMs composed of butanethiol (C4), heptanethiol (C7), dodecanethiol (C12), and octadecanethiol (C18) were selected to form a hydrophobic gradient (Fig. 3*A*). It is important to note that the contact angles of the C12 and C18 SAMs were similar to that of PDMS substrates (Table S2): between 100° and 110°. Additionally, an unmodified gold surface (Au) was incorporated as a control for the influence of the gold foundation on EB formation and a carboxylic acid-derivatized SAM, 16-mercaptohexadecanoic acid (MHA), was incorporated to test the influence of a hydrophilic terminal functional group (Fig. 3*A*).

Interestingly, as the surface hydrophobicity was augmented, enrichment for the intermediate size was observed (Fig. 3*B*). Moreover, the 18-carbon alkanethiolate SAM, which has a hydrophobic character similar to that of PDMS, offers the best surface for promoting efficient intermediate-size EB formation (Fig. 3*B*). Conversely, the majority of the aggregates counted on the more hydrophilic surfaces, including Au, MHA, and C4, were <100 μm in size.

The increasing surface hydrophobicity and contact angle also translated to a significant decrease in cell attachment (Fig. 3*C*, lower images). After 4 days of culture, the percentages of cell attachment under each culture condition were quantified and graphed against the respective surface contact angle. As demonstrated in Fig. 3*C Right*, hydrophobicity, or contact angle, is negatively correlated with cell attachment ($R^2 = 0.9514$). For example, the MHA surface, which is charged and hydrophilic under our culture conditions, promotes cell adherence and

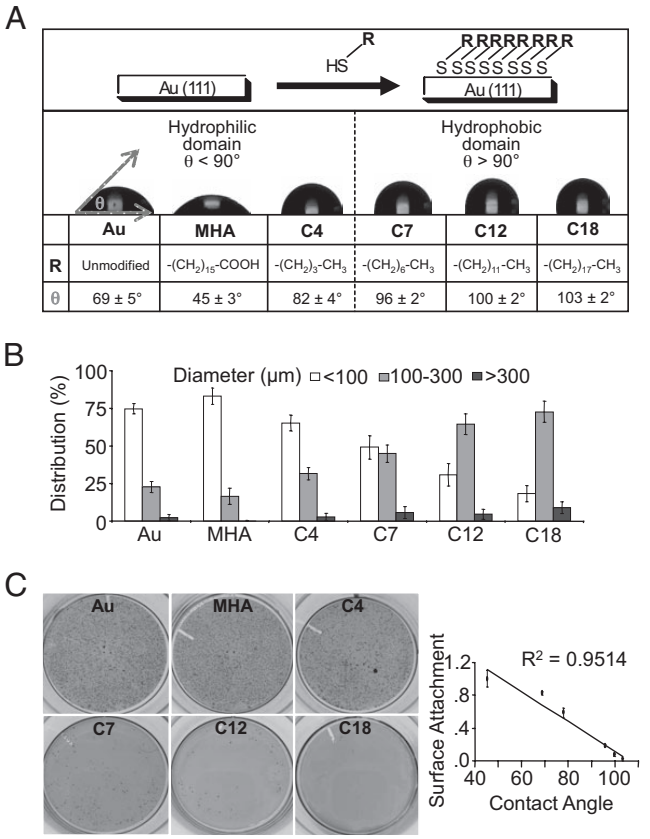

Fig. 3. Hydrophobic surfaces play a key role in the development of desired-size EBs. (*A*) Surface characterization of SAM films of alkanethiolates. *R*, terminal functional group; θ, water contact angle. (*B*) Day 4 EB size distribution on various surfaces, suggesting that an increase in surface hydrophobicity results in an enrichment of intermediate-size EBs. $n = 4$. (*C*) Negative correlation between surface attachment and contact angle. (*Left*) Cells in suspension were removed after 4 days of culture, and cells remaining on the surfaces were fixed and stained with crystal violet. (*Right*) Linear regression analysis was performed for the relationship between contact angle and cell surface attachment. $n = 3$.

produces the largest quantity of small EBs. In contrast, the most hydrophobic surface in our study, C18, impeded cell attachment and delivered the largest quantity of intermediate-size EBs. Overall, it appears that increasing surface hydrophobicity can positively influence EB growth and development while inhibiting cell-surface interaction and attachment.

Formation of Uniform-Size EBs from Human ES Cell Cultures. We next investigated whether the relationship between hydrophobicity and uniform EB formation holds true when applied to human ES cells. When HSF1 [University of California, San Francisco (UCSF)] human ES cells from the same stock were seeded on either LAC or C18 surfaces, we found that EBs cultured on C18 appear to be more uniform in size and morphology, as compared with LAC controls (Fig. 4*A*). Also compared with LAC cultures, human EBs formed on C18 surfaces display reduced cellular death (4.7% vs. 8.2%; $P \leq 0.01$; Fig. 4*B*) and enhanced cellular proliferation ($S/G_2/M$, 43.2% vs. 41.0%; $P \leq 0.01$; Fig. 4*C*). Similar to what was observed in the murine EB cultures, cell surface attachment was inhibited as hydrophobicity increased (Fig. S4). Collectively, it appears that human EB formation and development are also facilitated by hydrophobic surfaces, including C18 and PDMS (Fig. 4 and data not shown).

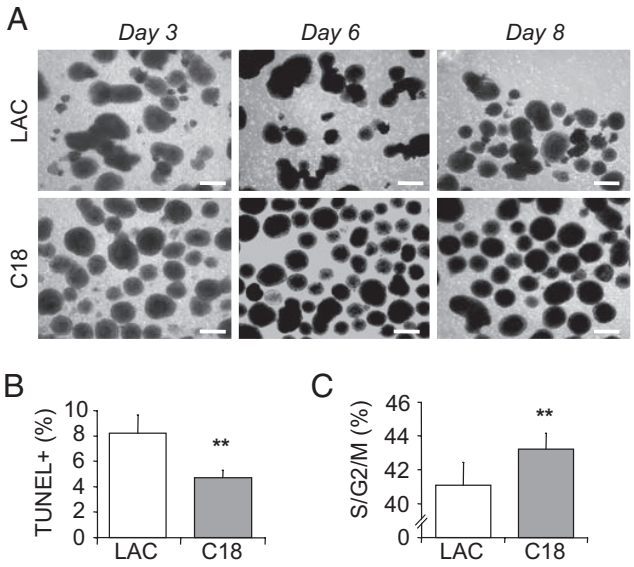

Fig. 4. Uniform human EB formation on hydrophobic surfaces. (*A*) Comparison of EBs derived from HSF1 human ES cells cultured either on LAC plates (*Upper*) or on C18 surfaces (*Lower*) and maintained in continuous culture for 8 days. (Scale bars, 250 μm.) (*B*) At day 7 of culture, EBs cultured on C18 display lower apoptosis profile as analyzed by TUNEL staining. $n = 5$. (*C*) A higher percentage of cells derived from EBs cultured on C18 resides in S/G_2/M after 7 days of culture. $n = 5$. Data presented as mean ± SD; **, $P < 0.01$.

PDMS Promotes Intermediate-Size EB Formation in the Absence of Serum. The aforementioned studies were carried out in the presence of fetal bovine serum (FBS), which is known to impact the efficiencies of EB formation and EB-mediated lineage differentiation (2). Additionally, most studies in the field are moving toward serum-free defined culture conditions with appropriate inducers (30). To test whether PDMS can promote intermediate-size EB formation in the absence of FBS, we first adapted LW1 ES cells to a serum-free culture system (ESGRO; Chemicon). After 15 passages in ESGRO medium, LW1 ES cells had fully adapted to the serum-free culture system and maintained their germ-line potential, the gold-standard of pluripotency (data not shown). These adapted LW1 ES cells were then passaged onto either LAC plates or PDMS-coated wells and cultured in ESGRO basal medium (Chemicon) without the key factors necessary for the maintenance of undifferentiated ES cell growth. Less cellular debris and cell death (32.5% vs. 16.4%, 12.3%, and 14.8%; Fig. S5 *A* and *B*) were observed on PDMS-coated wells, regardless of the soaking regimen. qRT-PCR analysis further revealed that EBs formed on PDMS in the absence of serum express the highest levels of genes associated with lineage differentiation ($P \leq 0.05$; Fig. S5*C*).

We next studied lineage-specific differentiation under defined conditions with appropriate inducers for each of the three somatic lineages and tested whether EBs formed on PDMS showed enhanced differentiation yields. When mouse and human ES cells were directed toward neuronal differentiation by means of EB intermediates (31), 2.4- and 1.6-fold increases in total number of neurons for mouse and human, respectively, were detected (Fig. 5*A* and Fig. S6*A*). We also detected significant increases when mouse and human EBs formed on PDMS were directed toward hematopoietic lineages (Fig. 5*B*) (31, 32). Similarly, when endoderm differentiation was attempted (31, 32), significant increases in gene expression associated with early- and late-stage endoderm differentiation were detected for both mouse and human when EBs were initially formed on a PDMS surface as compared with LAC plates (Fig. 5*C* and Fig. S6*B*). Collectively, by providing a more uniform population of intermediate-size EBs, PDMS serves as a suitable surface for promoting ES cell-mediated cellular proliferation and lineage differentiation, independent of FBS.

Discussion

To address whether EB size is a bona fide factor in determining differentiation efficiencies, we studied the first stage of EB development and demonstrated that EBs can be categorized into three subgroups according to their diameters: (*i*) aggregates (<100 μm) that are too small to develop into EBs; (*ii*) an agglomeration of several EBs that develop into large clumps (>300 μm), resulting in enhanced cell death; and (*iii*) aggregates of intermediate size (100–300 μm) for proper EB formation and development. Therefore, culture systems that can enrich for the intermediate-size EB population may significantly improve the yield of ES cell differentiation.

Our studies suggest that hydrophobic surfaces, such as those obtained from PDMS, C12, and C18, provide a local microenvironment that promotes the development of intermediate-size EB populations and inhibits cellular surface attachment. In

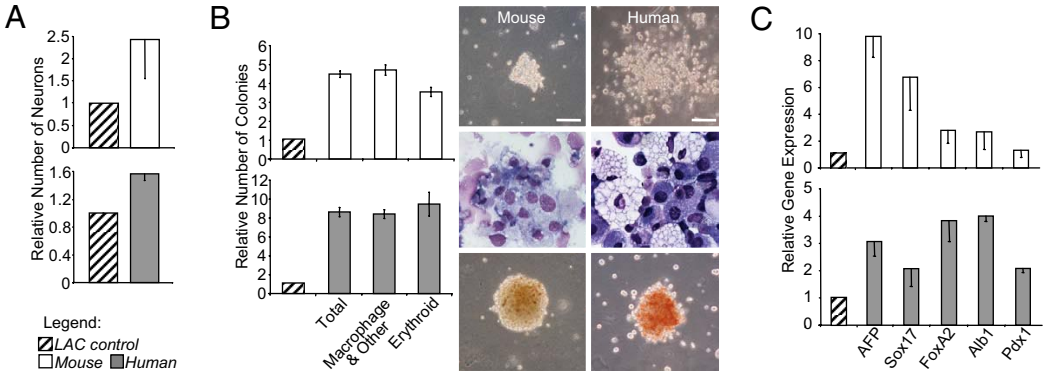

Fig. 5. Serum-free differentiation is enhanced by PDMS into the three somatic lineages. (*A*) Mouse and human ES cells were directed toward neuronal lineage for a total of 14 and 18 days, respectively, and scored for number of Tuj1 (neuronal marker)-positive cells under serum-free conditions. (*B Left*) Mouse and human ES cells were directed toward hematopoietic lineage for a total of 12 and 20 days, respectively, and scored for the appearance of various colonies in methylcellulose assay. (*Right Top*) Representative images of macrophage-containing colonies under brightfield microscopy for mouse and human. (*Right Middle*) The existence of macrophage colonies was confirmed by cytospin for mouse and human. (*Right Bottom*) Erythroid-containing colonies were confirmed by DAB staining for mouse and human. (Scale bars, 100 μm.) (*C*) Mouse and human ES cells were directed toward endoderm lineage for a total of 12 and 16 days, respectively, and assayed for associated gene expression. $n = 6$. Data presented as mean ± SD; all data, $P \leq 0.05$.

contrast, hydrophilic surfaces such as C4 or MHA could not inhibit surface attachment and produced mainly small aggregates. These observations suggest that SAMs designed for intermediate-size EB enrichment can be optimized by two parameters—(*i*) alkane chain length and (*ii*) chemical functionalities or terminal molecules presented at the culture interface—which, combined, ultimately govern surface wettability. For example, although MHA has a 16-carbon chain spacer, its carboxyl terminal group determines its wettability and produces EBs that are mainly of the small size.

Hydrophobic surfaces have previously been used as a nonadhesive background for cell patterning studies (33). Either PDMS or hydrophobic SAMs can serve as an efficient barrier for cell attachment over 1 week of cell culture (34). Compared with techniques that involve multistep procedures to immobilize inhibitory molecules like polyethylene glycol (35), PDMS-coated surfaces have the advantage of exhibiting naturally low adhesive character. Moreover, the fact that PDMS is widely used in microfluidic systems offers promising opportunities for large-scale culturing technologies. In addition to PDMS, hydrophobic SAMs can also support the formation of a monodispersed population of EBs derived from human ES cells. To better understand the contributions of PDMS to the observed enhancements in EB formation, we used attenuated total reflectance–Fourier transform infrared spectroscopy (ATR-FTIR) to analyze the nature of the culture surface. The resulting spectra indicate that proteins from the cell culture medium adsorb onto the surface of PDMS with no evidence of substrate degradation (Fig. S7). A more detailed analysis of the composition, texture, and mechanical response of this adsorbed film will be required in order to fully discern the role that substrate–media interactions play in contributing to the observed hydrophobicity-mediated enhancement in EB formation.

It is clear that the methyl-terminated hydrophobic surfaces studied here can provide significant benefits over currently used EB culture systems, with the production of uniform EB formation and enhanced cellular survival, proliferation, and differentiation. Importantly, our observations hold true regardless of FBS usage in the medium recipe, which will play a vital role as serum-free systems become the standard. In addition, PDMS can be readily applied as a coating for standard tissue culture plates. It does not require significant effort, added equipment, or experience in chemical synthesis for stem cell biologists who wish to carry out EB-mediated ES cell-lineage-specific differentiation studies. Collectively, these observations provide insight into the design of devices and culture systems intended for large-scale manufacturing of potential ES cell therapies.

Materials and Methods

PDMS. PDMS Sylgard 184 (Dow Corning) was prepared by mixing the prepolymer component with its cross-linker in a 10:1 weight ratio, in accordance with manufacturer recommendations. Surfaces for suspension culture of ES cells were then cast directly into six-well plates (Falcon) without degassing to form ≈2-mm substrates. Samples were then cured overnight at room temperature. For some cell lines, 1 mg/ml fresh BSA (MP Biomedical) solution was used to block residual and long-term culture adhesion to PDMS surfaces. Briefly, BSA was dissolved in Milli-Q water overnight at 4°C. The mixture was warmed in a 37°C water bath for 1 h, then heated in a 56°C water bath for 1 h. Next, it was filtered through a 0.22-μm PVDF filter (Steriflip; Millipore) and cooled at 4°C for 1–2 h. To coat, 2 ml of the BSA solution was added to each well and kept at 37°C overnight.

Preparation of SAM Substrates. Transparent gold-coated substrates were initially prepared in a clean-room facility (36). Glass coverslides (34-mm diameter; Fisher) were cleaned in a Piranha solution (70% H_2SO_4, 30% H_2O_2) at 100°C for 20 min, followed by thorough rinsing in DI water, and blown dry under a stream of nitrogen. Immediately after this cleaning procedure, a 10-nm layer of gold with a 5-nm titanium adhesion layer was deposited onto the cleaned cover glasses with a CHA E-beam evaporator. The result is an optically transparent, gold-coated substrate similar to materials reported elsewhere (36).

On completion of the gold evaporation, the slides were immediately transferred to our laboratory, where the samples were once again cleaned in Piranha at room temperature for 20 min and subsequently rinsed in DI water and blown dry with N_2. SAMs were then prepared by immersing the cleaned substrates in a 2 mM ethanolic solution of the appropriate alkanethiol overnight. Octadecanethiol (C18) samples were prepared using a 2 mM solution in 1-propanol for 2 days. On completion of the SAM formation, samples were removed from solution, rinsed with EtOH, and dried under a stream of N_2. The samples were then moved to the tissue culture facility, where they were inserted into six-well tissue culture plates. Before use, each well containing samples was washed three times with PBS (Gibco).

Additional Methods. The preparation of the various biocompatible surfaces, and the methods used, are described in *SI Materials and Methods*.

ACKNOWLEDGMENTS. We thank Drs. Kathrin Plath, Rudolf Jaenisch, Hanna Mikkola, and Laurraine Gereige, and members of our laboratories, for valuable suggestions. S.J.J. is supported by National Science Foundation Integrative Graduate Education and Research Traineeship: Materials Creation Training Program Grant DGE-0114443, University of California (Los Angeles) Medical Scientist Training Program, and the California NanoSystems Institute. O.N.W. is a Howard Hughes Medical Institute investigator. This work was supported by the National Institutes of Health (NIH) through NIH Roadmap for Medical Research Grant PN2 EY018228 (to H.W.).

1. Smith AG (2001) Embryo-derived stem cells: Of mice and men. *Annu Rev Cell Dev Biol* 17:435–462.
2. Keller G (2005) Embryonic stem cell differentiation: Emergence of a new era in biology and medicine. *Genes Dev* 19:1129–1155.
3. Robertson EJ (1987) *Teratocarcinomas and Embryonic Stem Cells: A Practical Approach* (IRL, Oxford).
4. Doetschman TC, Eistetter H, Katz M, Schmidt W, Kemler R (1985) The *in vitro* development of blastocyst-derived embryonic stem cell lines: Formation of visceral yolk sac, blood islands and myocardium. *J Embryol Exp Morphol* 87:27–45.
5. Bibel M, *et al.* (2004) Differentiation of mouse embryonic stem cells into a defined neuronal lineage. *Nat Neurosci* 7:1003–1009.
6. Keller G, Kennedy M, Papayannopoulou T, Wiles MV (1993) Hematopoietic commitment during embryonic stem cell differentiation in culture. *Mol Cell Biol* 13:473–486.
7. Keller GM (1995) *In vitro* differentiation of embryonic stem cells. *Curr Opin Cell Biol* 7:862–869.
8. Lumelsky N, *et al.* (2001) Differentiation of embryonic stem cells to insulin-secreting structures similar to pancreatic islets. *Science* 292:1389–1394.
9. Dang SM, Kyba M, Perlingeiro R, Daley GQ, Zandstra PW (2002) Efficiency of embryoid body formation and hematopoietic development from embryonic stem cells in different culture systems. *Biotechnol Bioeng* 78:442–453.
10. Chapman RG, *et al.* (2000) Surveying for surfaces that resist the adsorption of proteins. *J Am Chem Soc* 122:8303–8304.
11. Gouon-Evans V, *et al.* (2006) BMP-4 is required for hepatic specification of mouse embryonic stem cell-derived definitive endoderm. *Nat Biotechnol* 24:1402–1411.
12. Dang SM, Gerecht-Nir S, Chen J, Itskovitz-Eldor J, Zandstra PW (2004) Controlled, scalable embryonic stem cell differentiation culture. *Stem Cells (Dayton)* 22:275–282.
13. Ng ES, Davis RP, Azzola L, Stanley EG, Elefanty AG (2005) Forced aggregation of defined numbers of human embryonic stem cells into embryoid bodies fosters robust, reproducible hematopoietic differentiation. *Blood* 106:1601–1603.
14. Falconnet D, Csucs G, Grandin HM, Textor M (2006) Surface engineering approaches to micropattern surfaces for cell-based assays. *Biomaterials* 27:3044–3063.
15. Mohr JC, de Pablo JJ, Palecek SP (2006) 3-D microwell culture of human embryonic stem cells. *Biomaterials* 27:6032–6042.
16. Elisseeff J, Ferran A, Hwang S, Varghese S, Zhang Z (2006) The role of biomaterials in stem cell differentiation: Applications in the musculoskeletal system. *Stem Cells Dev* 15:295–303.
17. Engler AJ, Sen S, Sweeney HL, Discher DE (2006) Matrix elasticity directs stem cell lineage specification. *Cell* 126:677–689.
18. Hinz B, Celetta G, Tomasek JJ, Gabbiani G, Chaponnier C (2001) Alpha-smooth muscle actin expression up-regulates fibroblast contractile activity. *Mol Biol Cell* 12:2730–2741.
19. Tidwell CD, *et al.* (1997) Endothelial cell growth and protein adsorption on terminally functionalized, self-assembled monolayers of alkanethiolates on gold. *Langmuir* 13:3404–3413.
20. Darzynkiewicz Z, *et al.* (1997) Cytometry in cell necrobiology: Analysis of apoptosis and accidental cell death (necrosis). *Cytometry* 27:1–20.
21. Biswas A, Hutchins R (2007) Embryonic stem cells. *Stem Cells Dev* 16:213–222.
22. Carpenedo RL, Sargent CY, McDevitt TC (2007) Rotary suspension culture enhances the efficiency, yield and homogeneity of embryoid body differentiation. *Stem Cells (Dayton)* 25:2224–2234.
23. Thomson H (2007) Bioprocessing of embryonic stem cells for drug discovery. *Trends Biotechnol* 25:224–230.

24. Burridge PW, *et al.* (2007) Improved human embryonic stem cell embryoid body homogeneity and cardiomyocyte differentiation from a novel V-96 plate aggregation system highlights interline variability. *Stem Cells (Dayton)* 25:929–938.
25. Odorico JS, Kaufman DS, Thomson JA (2001) Multilineage differentiation from human embryonic stem cell lines. *Stem Cells (Dayton)* 19:193–204.
26. Pera MF, Trounson AO (2004) Human embryonic stem cells: Prospects for development. *Development* 131:5515–5525.
27. Schuldiner M, Yanuka O, Itskovitz-Eldor J, Melton DA, Benvenisty N (2000) Effects of eight growth factors on the differentiation of cells derived from human embryonic stem cells. *Proc Natl Acad Sci USA* 97:11307–11312.
28. Mikkola HK, Fujiwara Y, Schlaeger TM, Traver D, Orkin SH (2003) Expression of CD41 marks the initiation of definitive hematopoiesis in the mouse embryo. *Blood* 101:508–516.
29. Love JC, Estroff LA, Kriebel JK, Nuzzo RG, Whitesides GM (2005) Self-assembled monolayers of thiolates on metals as a form of nanotechnology. *Chem Rev* 105:1103–1170.
30. Murry CE, Keller G (2008) Differentiation of embryonic stem cells to clinically relevant populations: Lessons from embryonic development. *Cell* 132:661–680.
31. Irion S, *et al.* (2007) Identification and targeting of the ROSA26 locus in human embryonic stem cells. *Nat Biotechnol* 25:1477–1482.
32. Gadue P, Huber TL, Paddison PJ, Keller GM (2006) Wnt and TGF-β signaling are required for the induction of an *in vitro* model of primitive streak formation using embryonic stem cells. *Proc Natl Acad Sci USA* 103:16806–16811.
33. Orner BP, Derda R, Lewis RL, Thomson JA, Kiessling LL (2004) Arrays for the combinatorial exploration of cell adhesion. *J Am Chem Soc* 126:10808–10809.
34. De Silva MN, Desai R, Odde DJ (2004) Micro-patterning of animal cells on PDMS substrates in the presence of serum without use of adhesion inhibitors. *Biomed Microdevices* 6:219–222.
35. Kim P, *et al.* (2005) Fabrication of nanostructures of polyethylene glycol for applications to protein adsorption and cell adhesion. *Nanotechnology* 16:2420–2426.
36. Dimilla PA, *et al.* (1994) Wetting and protein adsorption of self-assembled monolayers of alkanethiolates supported on transparent films of gold. *J Am Chem Soc* 116:2225–2226.